Pis'ma v ZhETF, vol. 114, iss. 11, pp. 777 – 778

Double quantum dot FET on graphene

H. Mohammadpour[1)]

Department of Physics, Azarbaijan Shahid Madani University, 53714-161, Tabriz, Iran

Submitted 16 October 2021
Resubmitted 26 October 2021
Accepted 5 November 2021

DOI: 10.31857/S1234567821230099

Applications of quantum dots (QD) in electronic and optoelectronic devices rest beside the discrete energy levels of QDs [1–3]. Specially, QD-based nanoelectronic devices benefit from resonant tunneling of carriers via these levels that has wide applications in electronics [4–6]. Light-emitting FETs as well as phototransistors are modern devices that exploit the discrete energy levels of device [7–9]. Among the many devices are the graphene-based FETs [2, 10, 11]. Its unique physical and electronic properties, make graphene-based QDs promising candidates for quantum devices. In our previous works QD-channel on graphene FET was established by different engineering of the FET [2, 3]. QDs are also of interest as potential logic elements in future quantum computers [12, 13].

In the novel graphene-based Metal-Oxide-Semiconductor (MOS) FET model of this research, the gate electrode is not directly attached to the dielectric layer on top of the channel, but two separate metallic plates on top of dielectric layer cover two regions of channel. Then, a single metallic gate electrode is laid on top of the plates. Hence, the single gate electrode is equi-potential with the plates and turn them into gate electrodes with equal voltages.

By this geometry implementations, the gate voltage is applied to a set of two isolated QDs at the channel of the double-QD FET. The current-carrying region of the double-QD FET is on a single armchair graphene nanoribbon (A-GNR) with 13 carbon atoms in the width direction that has a band gap of 0.72 eV. The channel of FET which is controlled by the gate voltage is at the middle region of GNR and highly doped conducting source and drain regions of GNR are at the two sides of channel. The GNR, is sandwiched between two dielectric SiO_2 layers of dielectric constant $k = 3.9$ and 1 nm thickness.

The GNR-FET structure is symmetric at the top and bottom of GNR. The Fermi energy is transferred to the inside of conduction band only at the two quantum dots (QD-1 and QD-2).

Charge density of channel and current are computed by self-consistently solving 3-dimensional Poisson equation and the non-equilibrium Green's function (NEGF) formalism [14]. Real space tight-binding Hamiltonian is considered in nearest neighbor interaction approximation for atomistic p_z-orbital; $H = 2.7\Sigma_{i,j}\delta_{i,j\pm1}$ [15]. The retarded Green's function of device is defined as:

$$G(E) = [(E + i\eta)I - H - U - \Sigma_s - \Sigma_d]^{-1}, \quad (1)$$

where E is energy with I being a unit matrix and $\eta = 10^{-4}$ (eV) is a real number. U is the matrix of potential energy. The Hamiltonian matrix contains channel region of GNR and some unit cells of source and drain. The effects of semi-infinite source and drain GNR are included in left- and right-connected self-energies, $\Sigma_{L(or\,s)}$ and $\Sigma_{R(or\,d)}$ which are calculated according to the iterative algorithm described in [16].

The channel energy level broadening due to the source (drain) contact is $\Gamma_{s(d)} = i(\Sigma_{s(d)} - \Sigma^\dagger_{s(d)})$.

The matrix of potential energy, U at Eq. (1) is achieved by solving Poisson equation

$$\boldsymbol{\nabla}(\varepsilon\boldsymbol{\nabla}U) = e^2 n. \quad (2)$$

The electron density is calculated from electron correlation function, G^n as:

$$n = 2\int_{-\infty}^{+\infty} \frac{dE}{2\pi} G^n(E), \quad G^n = G\Sigma^{\rm in}G^\dagger \quad (3)$$

with the in-scattering function of contacts, $\Sigma^{\rm in}$, defined as:

$$\Sigma^{\rm in}(E) = \Gamma_s(E) f_s(E, E_{Fs}) + \Gamma_d(E) f_d(E, E_{Fd}) \quad (4)$$

$f_{s(d)}(E, E_{Fs(d)})$ is the Fermi–Dirac distribution function of source (drain) with Fermi energy equal to $E_{Fs(d)}$.

G^n is defined in terms of retarded Green's function $G(E)$ which is calculated from relation (1) using the recursive Green's function algorithm [17] provided that

[1)]e-mail: mhmdpour@gmail.com

potential matrix U is known. So, a self-consistent procedure for solving Eqs. (2), (3) is required.

The Landauer formula is employed for calculating current from the electron transmission function $T(E)$ as [14, 18, 19].

$$I = \frac{2e}{\hbar}\int_{-\infty}^{\infty} dET(E)(f_s(E) - f_d(E)),$$

$$T(E) = Tr[\Gamma_s G \Gamma_d G^{\dagger}]. \quad (5)$$

The GNR may be assumed as a one dimensional chain of rectangular unit cells of 0.43 nm width. Its characteristic lengths are: channel length, N_{Ch}, length of dots, N_{D1}, N_{D2}, the barrier between dots, N_B, and the barrier between channel and reservoirs, $N_R = 3$. The conduction and valence bands are plot for $N_{Ch} = 38$, $N_{D1} = 9$, $N_{D2} = 18$, $N_B = 5$ at the inset of Fig. 1 for $V_D = 0.1$ V.

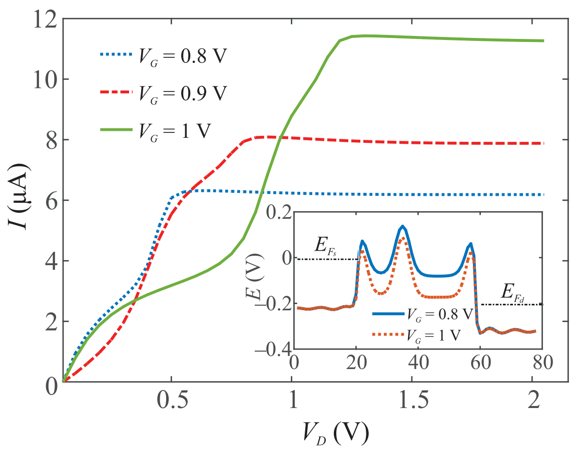

Fig. 1. (Color online) $I - V_D$ curves for various V_Gs and $N_{D1} = 12$, $N_{D2} = 15$, $N_B = 5$. Inset: Conduction and valence bands along channel of length scales, $N_{Ch} = 38$, $N_{D1} = 9$, $N_{D2} = 18$, $N_B = 5$ for $V_D = 0.1$ V and $V_G = 0.8$ V (solid), 1 V (dot)

There exist barriers at the two ends of channel adjacent to the contacts and a barrier is observed that divides channel into two QDs.

In the Figure 1 $I - V_D$ curves are plot for $N_{D1} = 12$, $N_{D2} = 15$, $N_B = 5$. The curves at the saturation region are larger for elevated values of gate voltages. However there is no linear region and in some drain voltage intervals current decreases for larger values of V_G.

At the next step a non-uniform behavior of the current with increasing V_G is observed. Current oscillates by increasing gate voltage.

In brief, at this research, a new design for GNR-FET is modeled in which the gate metal covers two separate regions of the channel layer. In this construction a quantum barrier is formed between the two regions and there are two barriers at the contact between the reservoirs (source and drain) to the channel. Quantum confinement of graphene channel by the barriers leads to formation of two QDs in the channel and hence gives rise to discrete energy levels. The calculated current is performed by resonant tunneling through these levels that is manifested by current versus gate voltage curves.

This is an excerpt of the article "Double Quantum dot FET on graphene". Full text of the paper is published in JETP Letters journal. DOI: 10.1134/S002136402123003X

1. M. Moradinasab, M. Pourfath, M. Fathipour, and H. Kosina, IEEES Trans. Electron Devices **62**(2), 593 (2015).
2. H. Mohamadpour and A. Asgari, Physica E **46**, 270 (2012).
3. H. Mohammadpour, Physica E **81**, 91 (2016).
4. J. Chen, M. A. Reed, A. M. Rawlett, and J. M. Tour, Science **286**(5444), 1550 (1999).
5. H. Agarwal, P. Kushwaha, J. P. Duarte, Y.-K. Lin, A. B. Sachid, M.-Y. Kao, H.-L. Chang, S. Salahuddin, and Ch. Hu, IEEE Transactions on Electron Devices **65**(5), 2033 (2018).
6. G. J. Ferreira, M. N. Leuenberger, D. Loss, and J. C. Egues, Phys. Rev. B **84**, 125453 (2011).
7. X. Chin, D. Cortecchia, J. Yin, A. Bruno, and C. Soci, Nat. Commun. **6**, 7383 (2015).
8. J. H. Schön, A. Dodabalapur, C. Kloc, and B. Batlogg, Science **290**(5493), 963 (2000).
9. D. Kim and J. Choi, Organic Electronics **51**, 287 (2017).
10. R. Li, L. Schneider, W. Heimbrodt, W. Heimbrodt, H. Wu, M. Koch, and Rahimi-Iman, Sci. Rep. **6**, 28224 (2016).
11. G. Konstantatos, M. Badioli, L. Gaudreau, J. Osmond, M. Bernechea, F. Pelayo Garcia de Arquer, F. Gatti, and F. H. L. Koppens, Nat. Nanotechnol. **7**, 363 (2012).
12. R. Akter, N. Islam, and S. Waheed, International Journal of Computer Applications **109**(1), 41 (2015).
13. V. K. Voronov, International Journal of Information, Technology and Computer Science **2**, 42 (2020).
14. S. Datta, *Quantum Transport: Atom to Transistor*, 2nd ed.,Cambridge University Press, Cambridge (2005).
15. K. I. Bolotin, K. J. Sikes, Z. Zhang, Zh. Jiang, M. Klima, G. Fudenberg, J. Hone, Ph. Kim, and H. L. Stormer, Solid State Commun. **146**(9/10), 351 (2008).
16. R. Lake, G. Klimeck, R. C. Bowen, and D. Jovanovic, J. Appl. Phys. **81** 7845 (1997).
17. M. P. Anantram, M. S. Lundstrom, and D. E. Nikonov, Proc. IEEE **96**, 1511 (2008).
18. R. Landauer, IBM J. Res. Dev. **1**, 223 (1957).
19. S. Datta, Superlattices and Microstructures **28**(4), 253 (2000).